ARTICLE OPEN

On the effect of Al on alumino-borosilicate glass chemical durability

Kamalesh Damodaran[1], Stéphane Gin[1✉], Sathya Narayanasamy[1] and Jean-Marc Delaye[1]

The chemical durability of borosilicate glass used to confine nuclear wastes is known to vary nonlinearly with their composition, making glass dissolution rate predictions difficult. Here, we focus on the effect of Al, an important oxide of these materials. The initial and residual glass dissolution rates were investigated through experiments conducted at 90 °C and pH 9. Our results show that low Al content glasses dissolve initially faster than glasses with higher Al content, but quickly achieve a lower residual rate due to the rapid formation of a more passivating gel. Nevertheless, the high Al content gel will eventually achieve passivation with a slower reorganization. The strengthening effect of Al on the Si-O bond hydrolysis will result in more stable gels, suggesting that slightly higher Al content in the gel will improve nuclear high-level waste glass durability in geological disposal conditions.

npj Materials Degradation (2023)7:46 ; https://doi.org/10.1038/s41529-023-00364-3

INTRODUCTION

The chemical durability of borosilicate glasses has been the subject of many studies ever since certain countries chose this material as a containment matrix for long-lived radioactive waste[1–3]. However, nuclear glasses are very complex materials (>20 oxides), and studying the reaction mechanisms between the glass and water demands working with simplified model materials. Therefore, since 2013, the scientific community has used a six-oxide borosilicate glass, called ISG glass, as the reference to establish a robust knowledge base concerning the dissolution mechanisms and kinetics of nuclear glasses[1,4,5]. In residual rate conditions, also called stage II alteration[6], ISG glass dissolution is slowed down by several orders of magnitude compared to the initial dissolution rate. This is because of an affinity reduction effect on the silicate network dissolution reaction, and by forming a passivating gel layer between the glass and the solution[7,8]. The physical and chemical processes at microscopic or even molecular scale that limits the residual rate remain to be established[7]. Many studies have focused on the formation and maturation of the passivating gel layers formed on nuclear glasses (for more details, see the following review articles by Frankel et al.[4], Gin et al.[5], and Thorpe et al.[9]). Diffusion properties of hydrous species in these gels depend on the composition of the glass and the solution (pH[10], concentration of Si and of some other elements such as big alkalis[11]), temperature, maturation time, and to a certain extent, on the glass structure. More precisely, short and medium structural order within the glass can differ depending on the cooling rate and the irradiation conditions[12,13]. The question of whether or not there is a link between the glass structure, the gel properties, and the residual rate still remains open[14]. Finding an answer would enable a better understanding of the passivating layer formation mechanism and thereby open the way to develop reliable kinetic models to predict these materials' long-term behaviors.

This study focuses on 6 Na-aluminoborosilicate glasses with Al_2O_3 content ranging from 0 to 6 mol%. Glasses are named SBNAx, where x corresponds to the mol% of Al_2O_3 in the glass. The formulation of these glasses does not follow a simple substitution rule, but still allows two-by-two comparisons i.e. each glass may be directly compared to at least one other glass. The initial dissolution rates were measured at 90 °C in a solution adjusted to pH 9 with LiOH, to determine the rate of matrix dissolution in the absence of both solution feedback effect and passivating layer. The rate drop related to solution feedback and passivation layer effects was studied with a 6-month static test conducted at a high glass-surface-area-to-solution-volume (SA/V) ratio in order to quickly achieve the silica saturation conditions necessary to form a passivating gel. Finally, a third experiment was conducted with a low Al content glass and a high Al content glass to investigate the passivation mechanisms of the gel layer. This experiment was carried out in a ^{29}Si spiked solution and solid-state characterization was performed with ToF-SIMS. Overall these experiments demonstrate that Al dramatically affects matrix dissolution and gel reorganization, with a huge impact on the glass dissolution rate.

RESULTS AND DISCUSSION

Initial dissolution rate

Figure 1 shows the evolution of the normalized mass loss of Si arising from the experiments conducted at 90 °C, pH 9, low SA/V ratio, and short duration (6 h). Initial dissolution rates, r_0, which correspond to the fastest dissolution rate for a given temperature and pH, are obtained by linear regression of the normalized mass loss. Note that, in this study, *NL*(Si) are calculated according to Eq. 1, using the BET surface area. Although a previous study[15] concluded that for powder, the actual reactive surface area is closer to the geometric surface area than the BET one. We made this choice to allow comparison with the long-term data, in which the BET surface area was predominantly used. The ratio between the BET surface area and the geometric one is close to 2 for all glasses (Table 1). Thus, this choice would not affect the comparisons among the glasses of this series, and thus the conclusions of the study. The values of r_0 are given in Fig. 1. Note that all the glasses dissolved congruently. The values of r_0 for the glasses SBNA0 and SBNA4 are in good agreement with literature data: 4.5 $g \cdot m^{-2} \cdot d^{-1}$ for CJ1 glass (equivalent to SNBA0) and 1.1 $g \cdot m^{-2} \cdot d^{-1}$ for glass CJ2 (equivalent to SBNA4) in Gin et al.[16]. Another study reports the same value for r_0(SBNA0)/r_0(SBNA4) of

[1]CEA, DES, ISEC, DPME, University of Montpellier, Marcoule, F-30207 Bagnols sur Cèze, Montpellier, France. ✉email: stephane.gin@cea.fr

4.5 ± 1, although the values for the two glasses are higher because the geometric surface area was considered in the study for normalization[17].

Regarding our series, there is a general trend showing a decrease of r_0 with increasing Al content in the glass (Supplementary Fig. 1). This trend is in agreement with a study involving 2669 glass compositions that demonstrated a similar effect of Al on the "PCT 7 days response", a normalized protocol that encompasses initial dissolution and rate drop regime[18]. Their results showed a non-linear response, with a positive effect of Al on glass durability up to 19 mol% of Al_2O_3. Further comparison is not possible, since the kinetic regimes investigated in the two studies are not same. In our series, since we did not follow simple substitution rules, only two-by-two comparisons are possible. Although SBNA0 does not contain Al, it dissolves slower than SBNA1 because the latter contains less Si and more Na. Comparison between SBNA1bis and SBNA3.5 is interesting because the two glasses have the same amount of Si and B. Only Na and Al differ. SBNA1bis dissolves 3.7 times faster than SBNA3.5. This effect can be attributed mostly to Al. Another comparison is possible between SBNA0 and SBNA4. The two glasses have similar $SiO_2 + Al_2O_3$ content and the same B_2O_3/Na_2O ratio (Supplementary Table 1). SBNA0 dissolves 4.9 times faster than SBNA4 confirming a major effect of Al. These results are in agreement with previous studies showing that Al increases glass durability in dilute medium[19,20]. Reiser et al.[21] discussed two possible mechanisms by which Al increases the durability of glass. (i) Al reduces the Na co-ordination with non-bridging oxygen (weak), and increases the Na co-ordination with Al (strong). (ii) Second mechanism proposes that Al increases the network connectivity of glass, which reduces the diffusion of water. A recent atomistic simulation study using molecular dynamics (MD) demonstrated that Al, being second neighbor to Si, increases the activation energy for dissociating the bonds around Si[22]. The authors also suggest that the diffusion of water might be reduced since the rate limiting step in an aluminosilicate glass is the dissociation of Si with four bridging oxygen atoms, whereas in a pure silicate glass, it starts with the dissociation of Si with only 3 bridging oxygen atoms. Such difference could delay the diffusion of water in aluminosilicate glass, which in turn modify the durability.

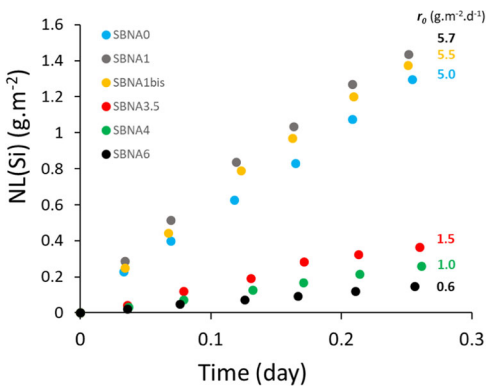

Fig. 1 Normalized mass loss of Si as a function of time. The slope obtained by linear regression provides the initial dissolution rate, r_0, measured at 90 °C in a solution adjusted to pH 9. Uncertainty on r_0 is ±30%.

180-day alteration experiments

These long-term static experiments were aimed at deciphering the role of Al on the concentration of silica at saturation, and glass dissolution rate drop. The experiments were conducted at high SA/V, 90 °C, and pH 9 for 6 months. As the reactors were placed in a second container filled with water, evaporation of the solution was negligible. In all the experiments, the pH remained stable over time and close to the target value (9.0 ± 0.2). Figure 2 shows the time dependence of the concentration of Si, *C(Si)*. In all cases, *C(Si)* readily increases, and eventually achieves a plateau characterized by stable, or slightly increasing concentrations, which can be considered as the saturation of the solution with respect to the gel. The plateau is reached at different *C(Si)*, depending on the glass composition. The three glasses with the lowest Al content (SBNA0, SBNA1, and SBNA1bis) have the highest *C(Si)* at saturation, between 400 and 500 $mg.L^{-1}$, whereas the glasses with increasing concentration of Al have lower *C(Si)* at saturation. Note also that the results for SBNA1 and its replicate (SBNA1_R) are similar.

As silica in a basic solution can dissociate, form oligomers, or complex with sodium, the Jchess geochemical code[23] was employed to calculate the activity of silica in the six solutions at three durations. Based on the measured *C(Si)*, the calculated saturation indices of amorphous silica in the solutions at three durations are shown in Fig. 3a. Figure 3b shows the effect of increasing Al_2O_3 concentration on the mean activity of silica in the solution. These calculations indicate that all the solutions remain undersaturated with respect to amorphous silica, but the degree of undersaturation increases with the content of Al in the glass. More precisely, the value of the plateau reached for each glass decreases linearly with the increase in the concentration of alumina in the glass (Fig. 3b). This result suggests that the presence of Al in the glass efficiently controls the release of Si into the solution due to the following reasons. The concentration of Si in solution results from both dissolution and condensation reactions. At equilibrium, the rate of the two opposite reactions are equal. The trend depicted in Fig. 3b agrees with recent atomistic simulations showing that Al as second neighbor of Si in aluminosilicate glass strengthens the Si (i.e. enhances the activation energy for dissociating Si–O bonds and decreases the activation energy for the Si-O bond reformation)[22]. Further calculations performed with different Molecular Dynamics (MD) techniques confirmed that the activation energies for bond

Table 1. Nominal compositions (mol%) of the six glasses designed to investigate the influence of Al on aluminoborosilicate glass, glass densities calculated from Fluegel's model[56], and geometric surface area and BET surface area of the powders used in this study. For the rate calculation, the BET surface area was used.

	SiO_2	B_2O_3	Na_2O	Al_2O_3	Density ($g.cm^3$)	S_{geo} 100–125 µm ($cm^2.g^{-1}$)	S_{BET} 100–125 µm ($cm^2.g^{-1}$)	S_{geo} 40–100 µm ($cm^2.g^{-1}$)	S_{BET} 40–100 µm ($cm^2.g^{-1}$)
SBNA0	67.8	18	14.2	0	2.42	220	405	354	690
SBNA1	63	18.7	17.3	1	2.46	217	355	348	645
SBNA1bis	60.5	20.1	18.4	1	2.46	217	415	348	720
SBNA3.5	60.5	20.1	15.9	3.5	2.40	222	415	357	715
SBNA4	64.9	17.3	13.7	4.1	2.39	223	435	359	720
SBNA6	66.8	15.9	11.3	6	2.36	226	455	363	780

dissociation and bond reformation are respectively larger and lower in aluminosilicate glass than pure silicate glass[24]. This means that aluminosilicate gels require less energy to form than pure silica gel. This result is in agreement with a lower solubility of aluminosilicate gel.

In the borosilicate glass alteration study, B and Na are usually selected to monitor the glass dissolution rate, especially when reverse reactions of condensation or precipitation control the net release of other glass constituents into the solution[5,7]. This choice assumes that B and Na released from the glass are not retained in any solid (gel, secondary phases). Therefore, the measurement of their concentration in the solution can be used to calculate the amount of reacted glass. In most cases, this assumption is presumed to be valid but is not verified. Recently, we demonstrated that (i) in some circumstances, B can be retained in the gel layer and that this retention could have a strong impact on the subsequent alteration of the glass[7], (ii) B diffusion coefficients in gels are low (~10^{-20} $m^2.s^{-1}$ in gel of ISG formed at pH 9)[25], (iii) B retention and diffusion in gels strongly depend on the pH and the presence of Ca[25].

Following this classical assumption that B can be used as a tracer, the equivalent thickness (*ETh(i)*) of the altered glass was calculated from B concentrations using Eq. 2, and plotted against the square root of time (Fig. 4). Note that the equivalent thicknesses of the altered glasses are given for all the elements in the Supplementary Fig. 2. Firstly, it is worth noting that the duplicated tests (SBNA1 and SBNA1-R) provide the same results, allowing us reliable comparisons among glasses of the series. Secondly, for a given glass, B and Na behave similarly, although the *ETh(i)* values for Na are lower than that for B in high Al content glasses. This suggests that Na could be retained in the gel to charge compensate four-fold coordinated Al atoms[26]. Thirdly, regarding B behavior, it appears that the three glasses with low Al contents dissolve rapidly during the first days and eventually achieve a very slow dissolution rate. Conversely, the three glasses with a higher Al content dissolve slowly at the beginning, but their dissolution rate diminishes extremely slowly. Moreover, for the two glasses with the highest Al content (SBNA4 and SBNA6), a linear release with square root of time is noticed, followed by a slower regime after ~80 days. For glass SBNA3.5, a continuous decrease of B release rate is observed.

Overall, the results of these long duration experiments show that the amount of Al in the glass strongly influences their behavior. The most durable glasses in Si-saturated conditions are those with a low concentration of Al, contrary to what is expected from the initial dissolution regime. To go further, we calculated the ratio between the initial dissolution rate, r_0, and the final rate obtained by linear regression between 110 days and 180 days. This ratio allows us to estimate the magnitude of the rate drop due to the formation of the gel layer. It is of the order of 4000 for SBNA0, >40,000 for glasses SBNA1 and SBNA1bis, 1000 for glass SBNA3.5, 200 for glass SBNA4, and 100 for glass SBNA6. These figures are valid only at a specific duration, as the residual rates of some of the glasses are still evolving even after 6 months. Nevertheless, they can still highlight the differences between glasses within the series. It is thus apparent that the glasses with low Al content form more passivating gels. The next experiment will try to better understand the reasons why.

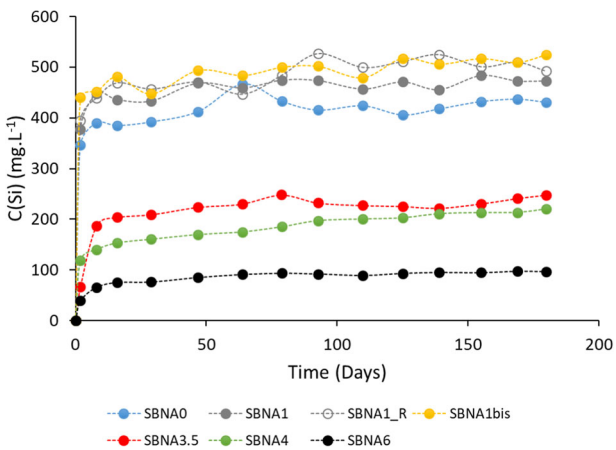

Fig. 2 Concentration of Si released into solution as a function of time. SBNA1_R is a replicate of SBNA1, conceived to verify the consistency of the dissolution experiments. Uncertainty is ±5%.

One month experiment

The 1-month experiment was conducted with two glasses, one from the low Al content glasses, SBNA1, and the other from the high Al content glasses, SBNA4. For this experiment, we used only glass coupons and performed ToF-SIMS depth profiling after the experiment. The leaching solution was enriched with $^{29}SiO_2$, close to the saturation with respect to amorphous silica and the pH was adjusted to 9.0 with LiOH. These conditions were chosen to ensure a rapid saturation of the solution with respect to the gel. Because of the low SA/V ratio selected for this experiment, it would have

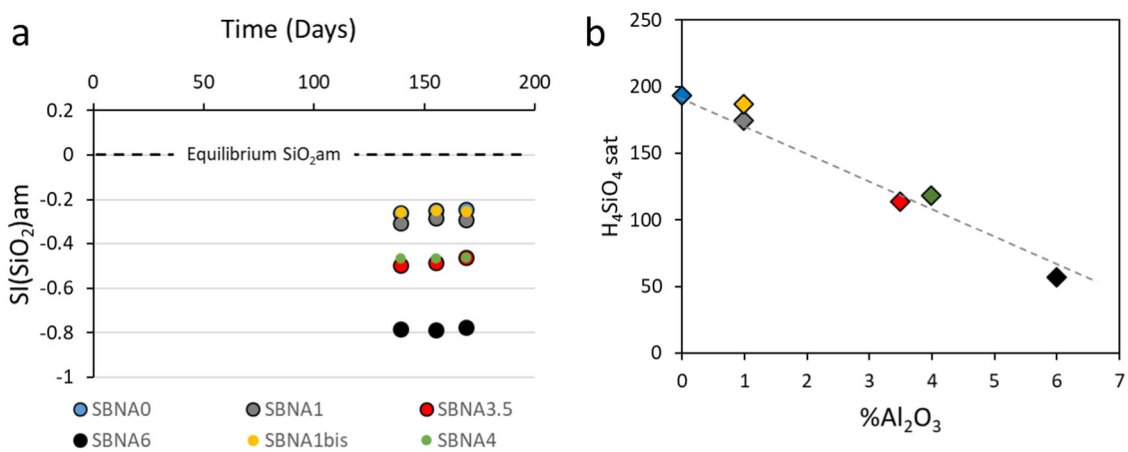

Fig. 3 Activity of silica in the long-term experiments. a Saturation indices of amorphous silica in the solutions with respect to time. **b** Correlation between the mean activity of silica in the solution vs concentration of Al_2O_3 in the SBNA series of glasses. The mean value is calculated between 139 days and 169 days. The linear regression of the correlation is displayed with dotted line ($[H_4SiO_4]sat = -23.08\ Al_2O_3 + 199.89$, $r^2 = 0.98$). The same color code is used for the different experiments.

taken a long time to reach the saturation state if the onset solution was free of Si. At the end of the experiment, the glass coupon was immersed for 24 h in ^{18}O labeled water. This tracing solution was free of Si but this second stage was conducted at room temperature to minimize subsequent gel and glass alteration. The equivalent thickness of altered glass was calculated from B and Na concentrations measured in the leaching solution (Fig. 5). The results show that SBNA1 glass corrodes incongruently (Na is released faster than B) and the dissolution rate dramatically drops beyond 10 days. Conversely, SBNA4 glass corrodes congruently and its dissolution rate remains almost constant over the experiment's duration. Note that Al concentrations were below detection limit. Compared to previous experiments conducted with glass powder, some differences are noticed:

- For SBNA1, B and Na are not released at the same rate, unlike in the long-term experiment. ToF-SIMS characterization will help understand the reason why B is released slower than Na.
- For SBNA4, B and Na are released at the same rate whereas some Na was retained in the gel in the long-term experiment.

Despite these differences, the altered glass thicknesses at the end of the 1-month experiment are similar to that determined with powder at the same duration. For the two studied glasses, the differences noted above can arise from the fact that the gel can form since the beginning of the reaction in the short term experiment due to the addition of silica in the starting solution, whereas the experiment with powder was started in a solution free of Si.

The ToF-SIMS depth profiles are presented in Fig. 6. First, it can be noticed that unlike SBNA4 glass, B is partly retained in the gel formed on SBNA1. The average retention is around 20% in the gel layer and the retention close to the gel-glass interface is around 30%. The retention of B in SBNA1 gel is the reason why the dissolution of this glass seems incongruent. Moreover, the amount of Na retained in the two gels is very small (around 10%), meaning that this element can be considered as a good dissolution tracer. As the transition between glass and gel is marked by the depletion front of B and Na, it is remarkable to see that the depletion fronts for B and Na are located at the same depth for each glass. This strongly suggests that Na release is limited by B dissolution, as it was already observed for ISG[7].

Despite the presence of 250 ppm of ^{29}Si in the solution, both gels keep the isotopic signature of the natural abundance (Fig. 6c, d). This result is a strong indication that the two glasses turn into gel by in situ hydrolysis/condensation reactions instead of dissolution/reprecipitation. As a reminder, this was shown in a previous study that an Al-free borosilicate glass similar to SBNA0 forms a gel by dissolution/reprecipitation[27]. Thus, considering the behavior of SBNA1, it seems that even a small amount of Al (here 1 mol% of Al_2O_3) could be sufficient to allow the gel to form by in situ hydrolysis/condensation. A major difference observed between the two glasses concerns $^{18}O/^{16}O$ ratio recorded in the gels (Fig. 6e, f). The $^{18}O/^{16}O$ ratio increases towards the glass in gel SBNA1 whereas it is almost flat and much lower in gel SBNA4. The blue line indicates the value of $^{18}O/^{16}O$ which should be achieved if all the porosity left by the release of B and Na is filled with ^{18}O labelled water. The way to calculate this curve is explained in a former paper[25]. For SBNA1 the porosity decreases toward the glass because of the retention of B in the gel. A counterintuitive result obtained with this tracing experiment is that the $^{18}O/^{16}O$ ratio increases with decreasing porosity.

There are two possible explanations to account for the result obtained with $H_2{}^{18}O$ tracing experiment. Either water molecules from the bulk solution fill the open pores and the result highlights the location of the open pores only, or these water molecules preferentially exchange their O atoms with that of the gel skeleton (OH groups, bridging oxygen (O_{br})) and do not fill all the pores. The first hypothesis suggests that closed pores mostly occupy the outer part of the gel, whereas the second hypothesis suggests that more reactive sites are located deeper in the gel, up to the reaction front. Looking at SBNA4 gel, the first hypothesis seems unlikely because the glass dissolution rate does not decrease, which means that the gel is not or poorly passivating at this reaction progress. A poorly passivating gel must consist of open pores. These pores must therefore be filled with $H_2{}^{18}O$. It is clearly not the case (Fig. 6f). The only possibility to keep this option open would be that pore water has evaporated during the ToF-SIMS analysis (due to the low pressure in the analysis chamber). One cannot totally rule out this option, but the analysis was run in cryogenic mode, and it has been confirmed that this mode

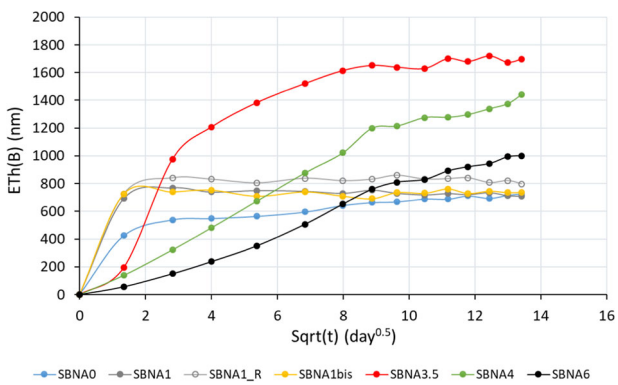

Fig. 4 Long term dissolution of B from SBNA series of glasses with respect to the square root of time. The color scheme for each glass are indicated appropriately.

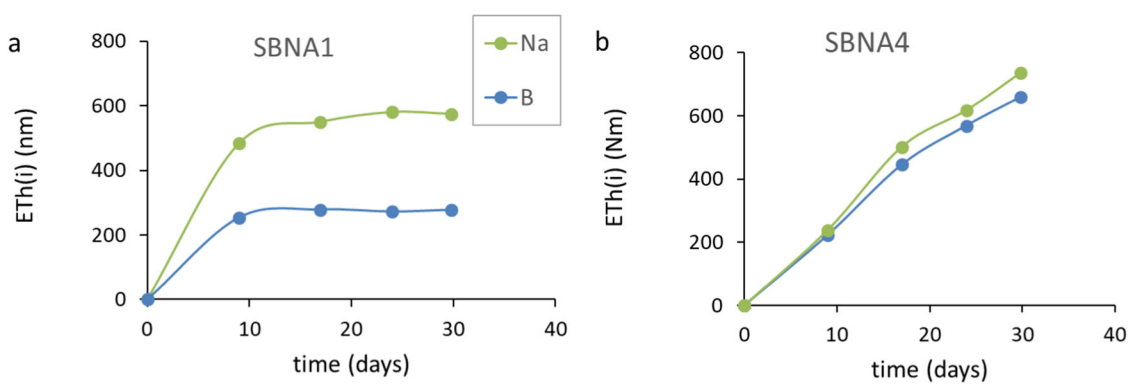

Fig. 5 B and Na dissolution from the SBNA glasses with respect to time for the 1-month experiment. a Equivalent thickness of B and Na for the SBNA1 glass. **b** Equivalent thickness of B and Na for the SBNA4 glass.

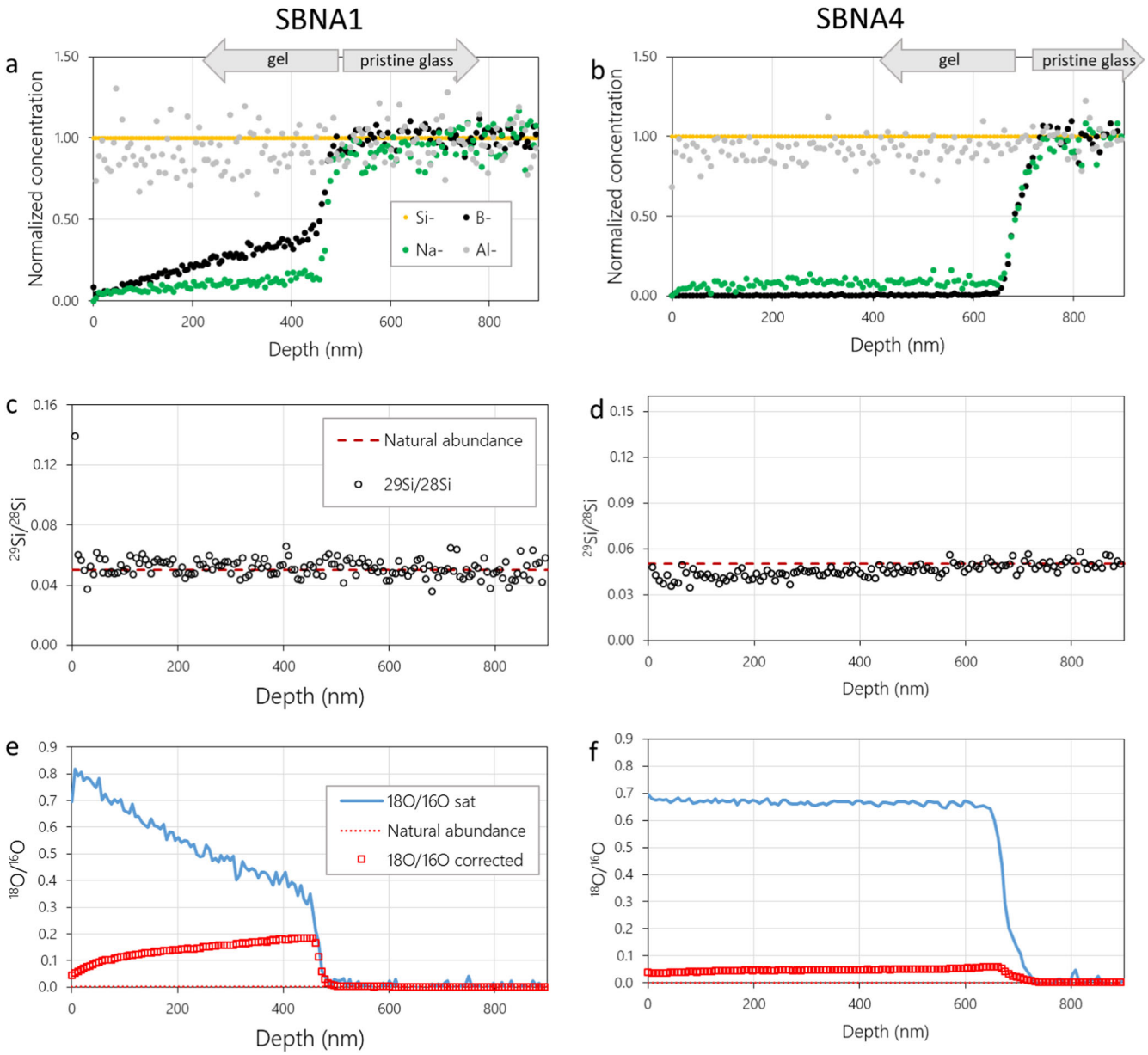

Fig. 6 ToF-SIMS analysis of SBNA1 and SBNA4 altered glass coupons. Experiments were conducted for 1 month in a Si saturated solution at 90 °C, followed by 1 day in $H_2{}^{18}O$ at room temperature. **a**, **b** B, Na, and Al profiles recorded in negative mode and normalized to Si. **c**, **d** $^{29}Si/^{28}Si$ profiles compared to the natural isotopic abundance (0.05) indicated as dotted line. **e**, **f** $^{18}O/^{16}O$ profiles (red squares) compared to that expected if the porosity left by the release of B and Na is saturated with ^{18}O labelled water (blue line). $^{18}O/^{16}O$ at natural abundance (0.002) is indicated as the red dotted line.

preserves most of the pore water during the analysis[28]. Therefore, it can be thought that some pores, even open, are not filled with labelled water. This hypothesis is supported by recent classical MD simulations with dissociative potentials for water molecules[29]. In this study, the authors introduced water in dry aluminosilicate gels containing pores[30]. The simulations showed that water molecules diffuse inside the gel skeleton and let some empty space within the pores. When these empty spaces are refilled with more water, the same phenomenon takes place, showing that the driving force let water molecules to enter the gel skeleton. This phenomenon is confirmed in another simulation study performed on amorphous silica nanotubes[31]. Thus, the signal recorded from ^{18}O tracing experiment would be more representative of the reactivity of the gel skeleton instead of the pore distribution. Following this idea, the correlation between B retention and ^{18}O enrichment suggests that O preferentially exchanges with O bound to B atoms. This hypothesis is in agreement with previous results showing a sharp increase of $^{18}O/^{16}O$ ratio in the inner region of ISG gels where B is trapped[14,32]. This is also supported by the conclusion obtained on ISG, which shows that in silica saturated conditions, glass dissolution is controlled by the breaking of B-O-Si linkages[7].

The case of SBNA1 is of great interest because its alteration ceases – or at least becomes extremely slow – during the course of the experiment and some B is detected in the gel. Recent work has shown that the retention of B in the gel impacts the continuation of the glass alteration reaction, not through water diffusion as it was suspected before[33] but more likely through further hydrolysis of B–O–Si linkages and diffusion of B_{aq}[25]. In that particular case, it can be proposed that the fast reorganization of the gel, highly permitted by the low concentration of Al, favors B

retention in the inner region of the gel, likely under aqueous form[34], which in turn dramatically reduce the rate at which glass continues to corrode. In that sense, gel reorganization appears to be a key step in glass protection by amorphous surface layer.

In this last section we discuss the implications of our findings. Borosilicate glasses are designed to contain large amounts of radionuclides (18 wt% of waste loading in R7T7 glass produced in France[35], up to 35 wt% of waste loading in some UK MW glasses[36]) while guaranteeing high resistance against irradiation and water[37–39]. According to our results, one can wonder if adding more Al into nuclear waste containment glasses could improve glass performance in geological disposal conditions. It is demonstrated that Al improves glass durability in the first kinetic regime (initial dissolution rate), whereas an opposite effect is observed in the residual rate regime as Al in glass delays the formation of the passivating gel. It is worth noting that these results are obtained in a simplified environment. Are they valid in a real disposal environment?

There is no unique and trivial answer to this question, because both the host rock and the materials in the vicinity of the glass could be reactive and thus could impact the mechanisms and kinetics of glass alteration[4]. For instance, it is known that Fe present in the primary canister and the overpack is soluble in anoxic and reducing environments, and could react with Si from the glass to form iron silicate minerals at the expense of the gel[40–46]. Furthermore, host rock can release porewater elements such as Mg and Ca, or organic acids that can react with the glass[11,47–50]. Often, reactions taking place between exogenous and glass elements decrease glass durability because many secondary and non passivating phases can form at the expense of the gel in the pH-T conditions of the disposal (typically 6 < pH < 9, 25 °C < T < 90 °C)[51]. There are thus larger uncertainties about the prediction of residual rate than initial dissolution rate, as precipitation of secondary phases mostly affect the residual rate regime. Such a mechanism is also known to trigger sudden resumption of alteration, also called stage III of glass corrosion[6,52,53]. A safe approach would then be to formulate glasses with the lowest possible initial dissolution rate. Consequently, extrapolating our findings to real disposal environment, it would be interesting to consider high Al content glasses.This will ensure the lowest reactivity in the presence of deleterious elements supplied by the environment. Another interest is that glasses with high Al content display lower concentrations of Si at saturation, which means that more stable gels (gels with lower solubility) can form. This is an advantage if gel formation competes with precipitation of secondary phases. These behaviors are more advantageous than quickly forming a passivating gel, as low Al content glasses do. Furthermore, the dissolution rate of the high Al content glasses tested in this study still diminish with time, meaning that the gel formed on these materials eventually become passivating. This was verified in a study conducted on ISG type glasses in which Si was substituted for Al[21]. Glasses with 0 to 22 mol% Al_2O_3, altered at 90 °C in static conditions with a SA/V ratio of 20 cm^{-1}, have similar residual rates calculated between 3 months and 13 months. The time scale that seems important in our laboratory studies becomes negligible on the storage time scale.

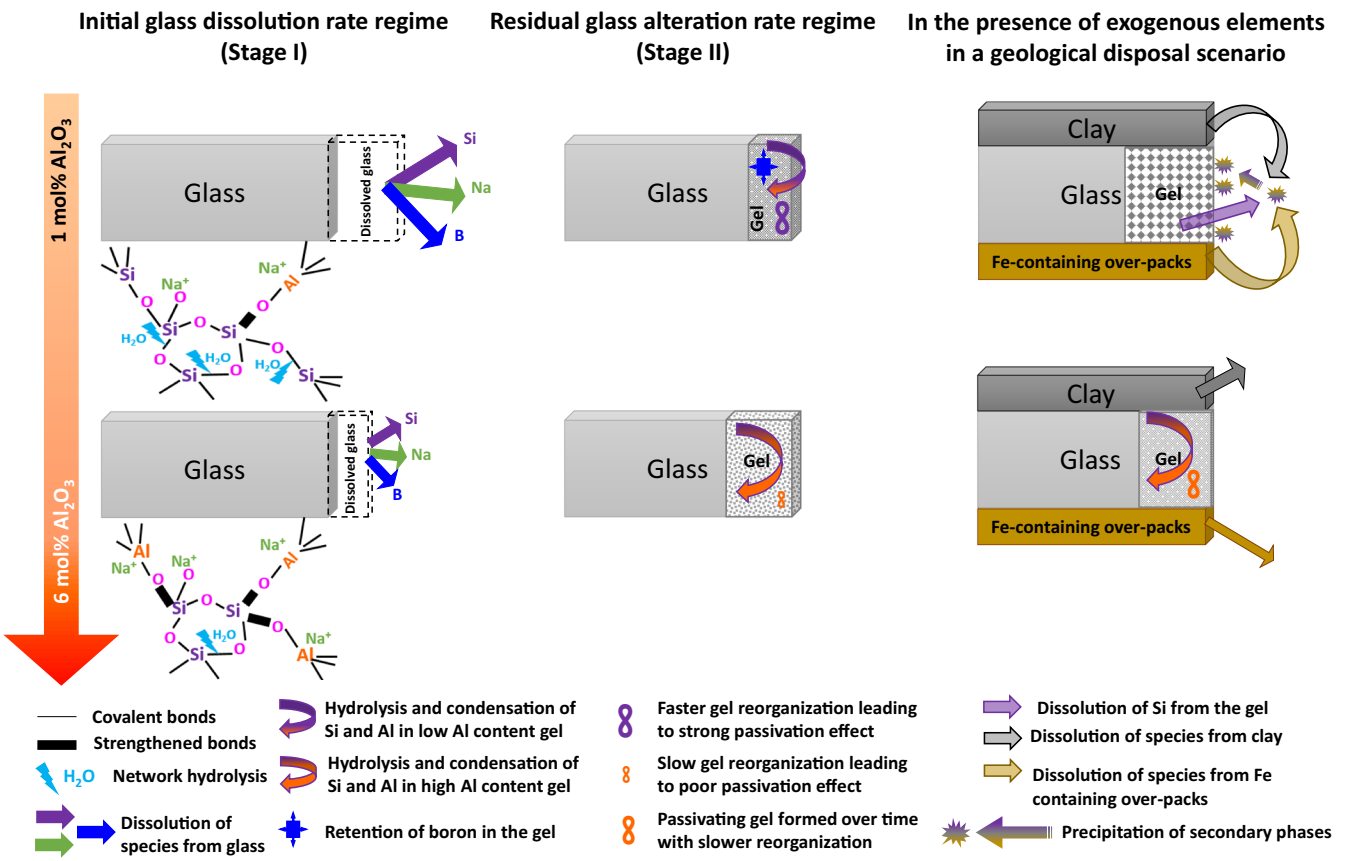

Fig. 7 A schematic description of the effect of Al in the glass on its durability in stage I and Stage II of glass alteration, and the extrapolation of our results in the lab scale to a geological disposal environment based on the comparison of our results with the literature. Briefly, high Al content in the glass reduces glass dissolution rate in stage I by stregthing the neighbouring Si-O- bonds against hydrolysis. But, it also inhibits rapid reorganization of the gel layer leading to initially poor passivating properties and higher residual glass alteration rate. Nevertheless, over time, they form more stable passivating gels that are less reactive in the presence of exogeneous elements.

The trends discussed above regarding the sensivity of the glass response to the environmental conditions have been confirmed by an experimental comparison between ISG (3.8 mol% Al_2O_3) and a peraluminous glass containing 15 mol% Al_2O_3[54]. Interestingly, the latter is significantly less susceptible to clayey groundwater and highly alkaline solutions[54]. The initial dissolution rate of this peraluminous glass is 2.5 times lower than that of ISG. The difference is significant but not huge because of the non-linear response of the glass upon composition variation[6,55].

In summary, Fig. 7 schematically describes the effect of Al in the glass on it's initial and final dissolution rates observed in this study and proposes an expected behavior in geological disposal conditions. It is clear that beyond the question of Al effect, the role of other elements, along with synergetic effects with other elements (Ca, Zr…) must also be considered. Although there is more work to do to define optimized glass compositions, the current study suggests that increasing Al content in peralkaline glasses or switching to peraluminous glasses would be two interesting options for the future.

METHODS

Glass preparation

Six Na-aluminoborosilicate glasses were studied. Nominal compositions are given in Table 1. Some key ratios between oxides are given in supplementary Table 1. Glasses are designed as SBNAx, where S stands for Si, B for B, N for Na, A for Al, and x the mol% of Al_2O_3 in the glass. For the 6 glasses the following procedure was applied. The mixture of raw materials (SiO_2, H_3BO_3, Na_2CO_3 and Al_2O_3) was introduced in a Pt-Rh crucible, then heated in a furnace at 1450 °C for 3 h and 20 min. The molten glass was then poured on a steel slab, then crushed after cooling and remelted at 1450 °C to ensure a good homogeneity. The resulting molten glass was poured into a graphite mold and annealed for 1 h at 550 °C. Glass composition was analyzed both by SEM-EDX (ZEISS MERLIN at CEA Marcoule, operating at 30 kV) for Si, Al and Na and ICP-OES (FILAB France) for all the elements after dissolution in acids. Both analytical techniques confirmed that actual composition match the nominal composition within analytical uncertainties (±5%).

From the annealed glass bars, small coupons with dimensions of $20 \times 20 \times 1$ mm^3 were cut with a diamond saw. The 6 faces of each coupon were polished up to diamond paste of 1 µm leading to a RMS < 5 nm. Glass powders of 100–125 µm and 40–100 µm size fraction were also prepared by the classical procedure of crushing, sieving and ultrasonic cleaning in ethanol and acetone to remove fine particles. The specific surface area of the two powders was measured by Brunauer, Emmett and Teller (BET) method using Kr gas (uncertainty ± 5%). The data are provided in Table 1.

Initial dissolution rate measurement

Initial dissolution rate of the 6 glasses was measured at 90 °C, pH 9 (at 90 °C) in static mode with glass powder. More details are given in a previous paper[17]. Briefly, 0.12 g of 100–125 µm powder is put in perfluoroalkoxy (PFA) vessel containing 400 mL of the leaching solution. The pH of the solution was adjusted with LiOH 1 M. Magnetic stirring ensures that glass particles did not lie at the bottom of the reactor. The 6 tests were conducted in parallel, using an oven regulated at 90 ± 2 °C. The solution was regularly sampled during the 6 h of the experiment. It is then acidified with diluted nitric acid and analyzed by inductively coupled plasma-optical emission spectrometry (ICP-OES, FILAB France).

From the elemental concentrations, normalized mass losses were calculated:

$$NL(i)_t = NL(i)_{t-1} + \frac{(C(i)_t - C(i)_{t-1}) \cdot V_t}{S \cdot x_i} \quad (1)$$

Where $C(i)_t$ is the concentration of element i in solution at the time t, V_t the volume of solution at time t, S the glass surface area determined from the BET specific surface area multiplied by the mass of glass, and x_i the mass fraction of the element i in the glass. $NL(i)$ is expressed in g.m^{-2}. The equivalent thickness, which gives the thickness of the glass that has been dissolved, based on the concentration of element i in solution, was calculated as follows:

$$ETh(i) = \frac{NL(i)}{\rho} \quad (2)$$

Where ρ is the density of the glass (Table 1).

Initial dissolution rate r_0 (g.m^{-2}.d^{-1}) is calculated in the linear regime from:

$$r_0 = \frac{d(NL(i))}{dt} \quad (3)$$

As r_0 refers to matrix dissolution, it is calculated from the release of Si. However, in this regime, glass dissolution is generally congruent, which means that the release rate of all glass cations is similar.

Concentrations, $NL(i)$, $ETh(i)$, and r_0 are given with 5%, 10%, and 30% uncertainty, respectively, according to Fournier et al.[15].

Long term experiments

The experiments were performed with the 6 SBNA glass powders. Experiments were conducted in 60 mL PFA vessels without magnetic stirring. Glass powder of mass ranging between 3.2092 to 3.8791 g were added to 50 mL of 18.2 MΩ.cm water whose pH was fixed at 9.0 ± 0.1 with 10^{-2} M LiOH solution, so that the initial glass-surface-area-to-solution-volume (SA/V) was 50 cm^{-1}. High SA/V ratio was chosen to quickly allow the solution to saturate with silica. To limit evaporation, the reactors were held in an over-pack container, also made of PFA and containing a few mL of deionized water. At each sampling duration, the reactor was dried, weighed and opened. Approximately 0.5 mL was taken with a syringe, filtered with a cutoff of 0.2 µm and diluted with 2 mL of 0.5 N ultrapure HNO_3 solution. Samples were collected every 7 days during first month and then every 15 days for the next 5 months. Collected samples were analyzed with Inductively coupled plasma-optical emission spectrometry (ICP-OES, FILAB France). Concentrations of Si, B, Na, and Al are given with an uncertainty of ±5%.

Normalized mass loss, equivalent thickness, and rate were calculated using Eqs. 1–3. In this case, as Si concentrations achieved quickly a plateau corresponding to a saturation state, B and Na are used as tracer for glass alteration.

Static, 1-month leaching experiments

For the 1-month tracer experiments, $^{29}SiO_2$ (Cortecnet, 99.69% of ^{29}Si) was dissolved in 18.2 MΩ.cm water adjusted to pH 9.0 ± 0.1 with 10^{-2} M LiOH solution to obtain 280 mg/L of ^{29}Si. A polished coupon was placed on a Teflon basket in a 20 mL PFA vessel with 14 mL of solution. Every 7 days 0.5 mL of solution was sampled and diluted with 2 mL of ultrapure HNO_3 solution. These samples were analyzed with ICP-OES (FILAB France) to measure the concentration of Si, B, Na and Al in the solutions. At the end of the experiment the glass coupon was recovered, quickly rinsed with ultrapure water and incubated in tracing solution containing 99% of $H_2{}^{18}O$ for 24 h at room temperature. After tracing, the monolith is taken out of the solution. The film of water is removed with pulsed dry air. The monolith is then plunged in liquid N_2 for 10 min before it is mounted on a cooled sample holder and instered in the vacuum chamber of the ToF-SIMS. ToF-SIMS depth profiling in both positive and negative modes was performed to investigate the depth wise ratio of $^{29}Si/^{28}Si$ and $^{18}O/^{16}O$ in the alteration layer. ToF-SIMS analysis was carried out in Tescan

Analytics, Fuveau, France using ToF-SIMS 5 spectrometer (Iontof—Münster, Germany), with the following conditions for positive mode: primary beam of Bi_1^+, 25 keV, I 0.2 pA with analyzed area of $50 \times 50\ \mu m^2$ and sputter beam of 1 keV, 300 nA of Cs^+ with abrasion area of $200 \times 200\ \mu m^2$. Similarly, ToF-SIMS conditions for negative mode were: Primary beam of Bi_3^{++}, 25 keV, 0.1 pA with analyzed area of $50 \times 50\ \mu m^2$ and sputter beam of 2 keV, 94 nA of Cs^+ with abrasion area of $200 \times 200\ \mu m^2$.

DATA AVAILABILITY

The data that support the findings of this study are available from the corresponding authors on reasonable request.

Received: 11 January 2023; Accepted: 12 May 2023;
Published online: 30 May 2023

REFERENCES

1. Gin, S. et al. An international initiative on long-term behavior of high-level nuclear waste glass. *Mater. Today* **16**, 243–248 (2013).
2. Grambow, B. Nuclear waste glasses—how durable? *Elements* **2**, 357–364 (2006).
3. Ojovan, M. I., Lee, W. E. & Kalmykov, S. N. *An Introduction to Nuclear Waste Immobilisation*. 3rd edn (Elsevier, 2019).
4. Frankel, G. S. et al. Recent advances in corrosion science applicable to disposal of high-level nuclear waste. *Chem. Rev.* **121**, 12327–12383 (2021).
5. Gin, S., Delaye, J.-M., Angeli, F. & Schuller, S. Aqueous alteration of silicate glass: state of knowledge and perspectives. *npj Mater. Degrad.* **5**, 42 (2021).
6. Vienna, J. D., Ryan, J. V., Gin, S. & Inagaki, Y. Current understanding and remaining challenges in modeling long-term degradation of borosilicate nuclear waste glasses. *Int. J. Appl. Glass Sci.* **4**, 283–294 (2013).
7. Gin, S. et al. Insights into the mechanisms controlling the residual corrosion rate of borosilicate glasses. *npj Mater. Degrad.* https://doi.org/10.1038/s41529-020-00145-2 (2020).
8. Neeway, J., Abdelouas, A., Grambow, B. & Schumacher, S. Dissolution mechanism of the SON68 reference nuclear waste glass: new data in dynamic system in silica saturation conditions. *J. Nucl. Mater.* **415**, 31–37 (2011).
9. Thorpe, C. L. et al. Forty years of durability assessment of nuclear waste glass by standard methods. *Npj Mater. Degrad.* https://doi.org/10.1038/s41529-021-00210-4 (2021).
10. Gin, S. & Mestre, J. P. SON 68 nuclear glass alteration kinetics between pH 7 and pH 11.5. *J. Nucl. Mater.* **295**, 83–96 (2001).
11. Collin, M., Fournier, M., Charpentier, T., Moskura, M. & Gin, S. Impact of alkali on the passivation of silicate glass. *Npj Mater. Degrad.* https://doi.org/10.1038/s41529-018-0036-3 (2018).
12. Angeli, F. et al. Effect of thermally induced structural disorder on the chemical durability of International Simple Glass. *npj Mater. Degrad.* **2**, 31 (2018).
13. Mir, A. H. & Peuget, S. Using external ion irradiations for simulating self-irradiation damage in nuclear waste glasses: State of the art, recommendations and, prospects. *J. Nucl. Mater.* **539**, 30 (2020).
14. Tribet, M. et al. New insights about the importance of the alteration layer/glass interface. *J. Phys. Chem. C.* **124**, 10032–10044 (2020).
15. Fournier, M. et al. Glass dissolution rate measurement and calculation revisited. *J. Nucl. Mater.* **476**, 140–154 (2016).
16. Gin, S., Beaudoux, X., Angeli, F., Jegou, C. & Godon, N. Effect of composition on the short-term and long-term dissolution rates of ten borosilicate glasses of increasing complexity from 3 to 30 oxides. *J. Non-Cryst. Solids* **358**, 2559–2570 (2012).
17. Gin, S. et al. Can a simple topological-constraints-based model predict the initial dissolution rate of borosilicate and aluminosilicate glasses? *npj Mater. Degrad.* **4**, 10 (2020).
18. Vienna, J. D. & Crum, J. V. Non-linear effects of alumina concentration on Product Consistency Test response of waste glasses. *J. Nucl. Mater.* **511**, 396–405 (2018).
19. Kim, D. S., Hrma, P., Palmer, S. E., Smith, D. E. & Schweiger, M. J. Effect of b2o3, cao, and al2o3 on the chemical durability of silicate glasses for hanford low-level waste immobilization. *Ceram. Trans.* **61**, 531–538 (1995).
20. Ledieu, A., Devreux, F. & Barboux, P. The role of aluminium in the durability of alumino-borosilicate glasses. *Phys. Chem. Glasses* **46**, 12–20 (2005).
21. Reiser, J. T. et al. Effects of Al:Si and (Al plus Na):Si ratios on the static corrosion of sodium-boroaluminosilicate glasses. *Int. J. Appl. Glass Sci.* **13**, 94–111 (2022).
22. Damodaran, K., Delaye, J. M., Kalinichev, A. G. & Gin, S. Deciphering the non-linear impact of Al on chemical durability of silicate glass. *Acta Mater.* **225**, 14 (2022).
23. van der Lee, J., De Windt, L., Lagneau, V. & Goblet, P. Module-oriented modeling of reactive transport with HYTEC. *Comput. Geosci.* **29**, 265–275 (2003).
24. Damodaran, K. *Insights Into the Mechanisms Controlling the Dissolution of Alumino-Borosilicate Glass and Development of a New Monte Carlo Model* (PhD Thesis, 2022).
25. Damodaran, K., Gin, S., De Montgolfier, J. V., Jegou, C. & Delaye, J. M. Behavior of B in passivating gels formed on International Simple Glass in acid and basic pH. *J. Non-Cryst. Solids* **598**, 9 (2022).
26. Angeli, F., Gaillard, M., Jollivet, P. & Charpentier, T. Influence of glass composition and alteration solution on leached silicate glass structure: A solid-state NMR investigation. *Geochim. Et. Cosmochim. Acta* **70**, 2577–2590 (2006).
27. Gin, S. et al. A general mechanism for gel layer formation on borosilicate glass under aqueous corrosion. *J. Phys. Chem. C.* **124**, 5132–5144 (2020).
28. Collin, M. et al. ToF-SIMS depth profiling of altered glass. *npj Mater. Degrad.* **3**, 14 (2019).
29. Taron, M. *Simulation à l'échelle Nanoscopique Du Transport Réactif: Application à La Dissolution Des Verres Nucléaires.* https://www.theses.fr/s218251 (2022).
30. Taron, M., Delaye, J. M. & Gin, S. A classical molecular dynamics simulation method for the formation of "dry" gels from boro-aluminosilicate glass structures. *J. Non-Cryst. Solids* **553**, 11 (2021).
31. Daub, C. D., Cann, N. M., Bratko, D. & Luzar, A. Electrokinetic flow of an aqueous electrolyte in amorphous silica nanotubes. *Phys. Chem. Chem. Phys.* **20**, 27838–27848 (2018).
32. Gin, S. et al. Origin and consequences of silicate glass passivation by surface layers. *Nat. Commun.* **6**, 8 (2015).
33. Gin, S. et al. Dynamics of self-reorganization explains passivation of silicate glasses. *Nat. Commun.* **9**, 9 (2018).
34. Kaya, H., Gin, S., Vogt, B. D. & Kim, S. H. Impact of aqueous solution pH on network structure of corrosion-induced surface layers of boroaluminosilicate glass. *J. Am. Ceram. Soc.* **105**, 6581–6592 (2022).
35. Vernaz, E. & Brueziere, J. In *2nd International Summer School on Nuclear Glass Wasteform—Structure, Properties and Long-Term Behavior (SumGLASS)* 3–9 (Elsevier Science Bv).
36. Fisher, A. J., Harrison, M. T., Hyatt, N. C., Hand, R. J. & Corkhill, C. L. The dissolution of simulant UK Ca/Zn-modified nuclear waste glass: the effect of increased waste loading. *MRS Adv.* **6**, 95–102 (2021).
37. Donald, I. W. *Waste Immobilization in Glass and Ceramic Based Hosts: Radioactive, Toxic and Hazardous Wastes* (Wiley, 2010).
38. Ojovan, M. I. & Lee, W. E. Glassy wasteforms for nuclear waste immobilization. *Metall. Mater. Trans. A-Phys. Metall. Mater. Sci.* **42A**, 837–851 (2011).
39. Gin, S., Jollivet, P., Tribet, M., Peuget, S. & Schuller, S. Radionuclides containment in nuclear glasses: an overview. *Radiochim. Acta* **105**, 927–959 (2017).
40. Michelin, A. et al. Effect of iron metal and siderite on the durability of simulated archeological glassy material. *Corros. Sci.* **76**, 403–414 (2013).
41. Dillmann, P., Gin, S., Neff, D., Gentaz, L. & Rebiscoul, D. Effect of natural and synthetic iron corrosion products on silicate glass alteration processes. *Geochim. Cosmochim. Acta* **172**, 287–305 (2016).
42. Guo, X. L. et al. Near-field corrosion interactions between glass and corrosion resistant alloys. *npj Mater. Degrad.* **4**, 15 (2020).
43. Guo, X. L., Gin, S. & Frankel, G. S. Review of corrosion interactions between different materials relevant to disposal of high-level nuclear waste. *npj Mater. Degrad.* **4**, 16 (2020).
44. Guo, X. L. et al. Self-accelerated corrosion of nuclear waste forms at material interfaces. *Nat. Mater.* **19**, 310–316 (2020).
45. Schlegel, M. L. et al. Alteration of nuclear glass in contact with iron and claystone at 90 degrees C under anoxic conditions: Characterization of the alteration products after two years of interaction. *Appl. Geochem.* **70**, 27–42 (2016).
46. Michelin, A. et al. Silicate glass alteration enhanced by iron: origin and long-term implications. *Environ. Sci. Technol.* **47**, 750–756 (2013).
47. Mann, C. et al. Influence of young cement water on the corrosion of the International Simple Glass. *npj Mater. Degrad.* **3**, 9 (2019).
48. Fisher, A. J. et al. Short communication: the dissolution of UK simulant vitrified high-level-waste in groundwater solutions. *J. Nucl. Mater.* **538**, 7 (2020).
49. Gin, S., Godon, N., Mestre, J. P., Vernaz, E. Y. & Beaufort, D. Experimental investigation of aqueous corrosion of R7T7 nuclear glass at 90°C in the presence of organic species. *Appl. Geochem.* **9**, 255–269 (1994).
50. Jollivet, P. et al. Effect of clayey groundwater on the dissolution rate of the simulated nuclear waste glass SON68. *J. Nucl. Mater.* **420**, 508–518 (2012).
51. Jantzen, C. M., Trivelpiece, C. L., Crawford, C. L., Pareizs, J. M. & Pickett, J. B. Accelerated Leach Testing of Glass (ALTGLASS): II. Mineralization of hydrogels by leachate strong bases. *Int. J. Appl. Glass Sci.* **8**, 84–96 (2017).
52. Ribet, S. & Gin, S. Role of neoformed phases on the mechanisms controlling the resumption of SON68 glass alteration in alkaline media. *J. Nucl. Mater.* **324**, 152–164 (2004).

53. Gin, S. et al. The fate of silicon during glass corrosion under alkaline conditions: a mechanistic and kinetic study with the International Simple Glass. *Geochim. Cosmochim. Acta* **151**, 68–85 (2015).
54. Piovesan, V. et al. Chemical durability of peraluminous glasses for nuclear waste conditioning. *npj Mater. Degrad.* **2**, 10 (2018).
55. Frugier, P., Martin, C., Ribet, I., Advocat, T. & Gin, S. The effect of composition on the leaching of three nuclear waste glasses: R7T7, AVM and VRZ. *J. Nucl. Mater.* **346**, 194–207 (2005).
56. Fluegel, A. Global model for calculating room-temperature glass density from the composition. *J. Am. Ceram. Soc.* **90**, 2622–2625 (2007).

ACKNOWLEDGEMENTS

This study was supported as part of the center for Performance and Design of Nuclear Waste Forms and Containers, U.S. Department of Energy (DOE) [Award #DESC0016584].

AUTHOR CONTRIBUTIONS

S.G. supervised the study and wrote the paper. K.D. ran the experiments. All the authors participated to the scientific discussion and contributed to the editing of the manuscript under its present form.

COMPETING INTERESTS

The authors declare no competing interests.

ADDITIONAL INFORMATION

Supplementary information The online version contains supplementary material available at https://doi.org/10.1038/s41529-023-00364-3.

Correspondence and requests for materials should be addressed to Stéphane Gin.

Reprints and permission information is available at http://www.nature.com/reprints

Publisher's note Springer Nature remains neutral with regard to jurisdictional claims in published maps and institutional affiliations.

Open Access This article is licensed under a Creative Commons Attribution 4.0 International License, which permits use, sharing, adaptation, distribution and reproduction in any medium or format, as long as you give appropriate credit to the original author(s) and the source, provide a link to the Creative Commons license, and indicate if changes were made. The images or other third party material in this article are included in the article's Creative Commons license, unless indicated otherwise in a credit line to the material. If material is not included in the article's Creative Commons license and your intended use is not permitted by statutory regulation or exceeds the permitted use, you will need to obtain permission directly from the copyright holder. To view a copy of this license, visit http://creativecommons.org/licenses/by/4.0/.

© The Author(s) 2023, corrected publication 2023